The features and spatial distribution of loessic soils around Mt. Canobolas in the New South Wales Central Tablelands

Brendan P. Malone

Sciences Discipline, Faculty of Agriculture, Food and Natural Resources,
The University of Sydney, NSW 2006, Australia.

Abstract. Australia's vast arid and semi-arid landforms represent major potential sources for aeolian dust. Dust deposition has been a significant factor in the pedogenesis of many soils, particularly throughout the south east of the continent where 'parna', the aggregated clayey, calcareous aeolian material has dominated our perception of dust processes. More recently, however, this understanding has expanded with the discovery of aeolian deposits different in composition and distribution to that of 'parna'.

Using granulometric, mineralogical and micromorphological techniques to characterise a number of soils around Mt Canobolas in the NSW Central Tablelands, there is now compelling evidence that some topsoils in the area are comprised of deposited aeolian dust that display characteristics more typical of silty 'loess'. Where these loessic topsoils exist, they are lithologically and morphologically distinct from the predominantly basalt derived soils in the area. The loessic silt has negligible clay content, but is dominantly composed of particles enriched with quartz and K-feldspar minerals that have a modal diameter of 35–42 μm.

The spatial distribution of the loessic soils was predicted with a nominal logistic model. It appears that the uplifting of Mt Canobolas and the surrounding area have create a significant barrier to the path of suspended dust that has travelled from tens to a thousand or more kilometres from its source, presumably in central western or western NSW. These loessic soils are predicted to be widespread, found only at higher elevations and exist as thin mantles on the crests of gentle slopes or as thick deposits in topographic lows. However, with only a fair agreement between actual loessic sites and modelled predictions (Kappa = 0.35), further improvements to the predictive model could be made. Nonetheless, in the future, a similar framework could be applied in other locations where dust accession is thought to occur.

Additional keywords: aeolian dust, dust deposition, loessic soils, loess distribution

Introduction

The Australian continent is composed predominantly of arid and semi-arid landforms including dune fields, playa lakes, and dry floodplains. These areas represent major potential sources for aeolian dust of which have been a significant factor in the pedogenesis of many soil landscapes throughout the continent (Bowler 1976; Hesse and McTainsh 2003). Aeolian dust is regarded as a suspension of wind-blown particles no greater than 100 µm in the earth's atmosphere, or a deposit of such particles onto the land (Pye 1987). The universal name used to describe these deposits is 'loess', which is defined classically as; 'the terrestrial clastic sediment, composed predominantly of silt-sized particles, which formed essentially by the accumulation of wind-blown dust' (Pye 1995). It has also been more broadly defined as; 'all aeolian deposits where transport has been primarily by suspension, irrespective of content of organic matter, mineralogical composition, calcium carbonate content, degree of compaction or texture' (Raeside 1964).

In the past, there has been an element of conjecture as to the presence of 'loessic' soils in Australia, possibly because deposited dust does not occur as thick loess mantles as it does in other parts of the world. Additionally, the fundamental principle of loess formation is that it is inherently linked to glaciation processes, which have had only a limited impact on the Australian continent (Barrows 2001). Also at odds with the classic loess definition is the seminal work of Butler (1956), who pioneered the principle model of aeolian dust deposits in south eastern Australia. He described a calcareous, red-clay material of aeolian origin as 'parna', which at the time, did not fit with the existing definitions of loess. While there have been further studies in describing 'parna' and 'parna-like' deposits (Beattie 1970; Chen 2001), there is a growing acceptance that 'parna', rather than being relegated as a scientific curiosity, actually displays characteristics similar to that of aeolian dusts derived from 'hot' or desert loess forming processes. These are conventionally termed as 'desert loess' or 'loessic-clays' (Dare-Edwards 1984; Haberlah 2007).

Butler (1956) asserted that 'parna' exists in various topographic situations throughout southern NSW and northern Victoria (Butler 1956; Beattie 1970; Chen 2001). However, discoveries in recent times have shown that the distribution of loessic soils in south eastern Australia are considerably more widespread and compositionally distinct from 'parna' (Hesse and McTainsh 2003). For example, Cattle *et al.* (2002) and Tate *et al.* (2007) in northern and north western NSW respectively, identified and characterised dust deposits as containing more quartz and less clay compared with the 'parna' described by Butler (1956). Cattle *et al.*

(2002) reported that the modal diameter of the quartz-rich dust particles ranged between 40–50 µm, while Tate *et al.* (2007) reported that highly abraded 70 µm quartz grains were characteristic features of the dust in their study area in western NSW. In the NSW Central Tablelands, Humphreys *et al.* (2002) described the presence of classically defined loess mantles near Blayney that bore little resemblance to 'parna' and were dominated by silt-sized quartz (10–50 µm) and lesser amounts of clay minerals such as kaolin and mica. These studies and others highlight that the variation in deposited dust features throughout south eastern Australia are inherently attributed to the varied nature of, and distance from, dust source areas (Hesse and McTainsh 2003).

In the area around Mt Canobolas, near Orange in the NSW Central Tablelands there is anecdotal evidence that some soils display 'loessic' characteristics. In areas where water-borne sediment is not possible, grey-brown top soils are significantly lighter in texture compared to the sub-soils, they are also poorly structured, very dispersive and overall, problematic to manage in an agricultural setting. These are confounding properties when considering that geologically, much of this area is underlain by Tertiary volcanic basalts rocks that upon weathering have formed moderately fertile, strongly structured and texturally uniform soils (Kovac and Lawrie 1990). They also have an abundance of clay and a strong iron-stained colouring.

Possibly the greatest limitation with characterising dust affected soils is that the data reveals only point-specific information about their location in a study area. In order to further our understanding of aeolian dust deposition as a pedogenic process, it is equally important to be able to define the spatial distribution of loessic soils in the wider landscape. In efforts to do so, previous studies by Chen (2001) and Summerell *et al.* (2000) have used independent methods of describing and mapping the presence of aeolian deposits in expansive study areas. Chen (2001) used a combination of soil survey and soil landscape maps to define the distribution of 'parna' with respect to different landform types around Wagga Wagga, NSW, while Summerell *et al.* (2000) developed a conceptual model of 'parna' deposition and landform capacity for retaining the sediment using a digital elevation model and derived terrain indices to identify the spatial distribution of 'parna' in hilly terrain around Young, NSW.

Therefore, the aims of this study are to *i*) identify and characterise the granulometric, mineralogical and micromorphological properties of soils at three sites near Mt. Canobolas where dust accession has thought to have occurred; *ii*) to verify that this suspected loessic

material has an aeolian origin, and; *iii*) to develop a predictive model that will determine the spatial distribution of the loessic material in the immediate area surrounding Mt. Canobolas.

Materials and methods

The Mt Canobolas study area and study sites

Mt Canobolas (33°20'39"S, 148°58'56"E) is situated in the NSW Central Tablelands about 13 km west-south-west of Orange, which itself is 250 km west of Sydney, NSW. An extinct volcano, Mt Canobolas, is a prominent landform in the area with an elevation of 1396 m a.s.l.

Geologically, the basement rocks in the area comprise of uplifted Palaeozoic volcanics and sediments that have been intruded by Carboniferous granitoids (Scott 2003). During the late Tertiary (13–11 Ma), lava from Mt Canobolas radiated outwards and blanketed the landscape forming extensive lava plains and inverted lava flows. These Tertiary volcanic units are composed predominantly trachytes and alkali rhyolites , as well as significant units of olivine basalts and minor units of porphyritic andesine basalts. (Pogson and Watkins 1998). Subsequent weathering of the Tertiary Volcanics has resulted in areas of moderately fertile, iron-stained and kaolin rich soils (Scott 2003). In the Soil Landscapes of the Bathurst 1:250 000 Sheet, Kovac and Lawrie (1990) describes these soil types as Krasnozems (Stace *et al.* 1968) or Red Ferrosols in the Australian Soil Classification (ASC) system (Isbell 1996).

The climate of the area is temperate with a mean annual rainfall of around 885 mm. At Orange, the mean daily maximum and minimum temperatures are 17.6°C and 6.2°C respectively (Bureau of Meteorology 2008).

Three study sites were chosen where aeolian material has been suspected of occurring within the landscape (D. McKenzie, pers comm. 2008). Coincidently, these sites are also located in the areas where the basaltic rock and soil units exist (Pogson and Watkins 1988; Kovac and Lawrie 1990). It was anticipated that the underlying basalt-derived soil would be lithologically distinct from the likely aeolian material, thus aiding identification and characterisation.

At each study site, observations were made of the locality of the suspected aeolian material and nearby locations where it does not exist. As such, paired sites were determined and soil samples were collected during soil pit excavation or with a hand auger.

Site 1

'Caldwell' (33°16'2"S, 148°59'57"E) is located about 11 km west of the Orange CBD. The property is a vineyard situated upon gently undulating land in the mid-slope area north of Mt Canobolas, approximately 880 m a.s.l. The site where the suspected aeolian material exists is located on the crest of a gentle slope with a north-facing aspect. A soil pit was dug, exposing three distinct horizons; a structureless grey silt loam horizon to 0.2 m (BD–D1); to a mixed layer of suspected dust and red clay that had little structure and light clay field texture to 0.45 m (BD–D2); to a more-or-less

whole coloured red clay horizon with a light-medium clay field texture and strong granular structure to > 0.8 m (BD–D3). Samples were collected from each of the horizons for further analysis.

The paired site was located nearby on the same hill but with an easterly aspect. A hand auger was used to collect two samples; at 0–0.1 m the soil was a red/brown silty clay loam (BD–B1); and between 0.4–0.5 m where the soil was a whole coloured red, light-medium clay (BD–B2).

Site 2

'Nashdale' (33°17'54"S, 149°1'14"E) is a vineyard property located about 7 km west-south-west of the Orange CBD. Within close proximity to Mt Canobolas, the topography in the general vicinity of the property is defined as the upper to mid slope area that is dominated by gentle to medium sloped rolling hills about 930 m a.s.l. The site where the suspected aeolian material exists is on bare ground adjacent to wine grape vines on the crest of a very gentle south westerly facing slope. Using a hand auger, two samples were collected; at 0–0.15 m where the soil was a grey-brown colour with a silt-loam field texture (LC–D1); and between 0.4–0.5 m where the soil had a bright orange-red colouring with light clay field texture (LC–D2).

The paired site was located nearby between grape vines on the same crested area but with an easterly aspect. A hand auger was used to collect two samples; at 0–0.1 m the soil was a light reddish brown colour with a silty clay field texture (LC–B1); and between 0.4–0.5 m where the soil was a dark orange-red colour with a light clay field texture (LC–B2).

Site 3

'Towac' (33°18'51"S, 149°2'37"E) is a small hobby farm located on the upper-sloped area of Mt Canobolas about 6 km south-west of the Orange CBD. The property itself is situated within a lower lying region of the upper sloped area that is flanked by gentle to medium sloped rolling hills in all directions about 970 m a.s.l. The site where the suspected aeolian material exists is between grape vine rows on very gently sloping land with a southerly aspect. A soil pit was dug to 0.75 m to reveal three distinct soil horizons from which samples were taken; a distinct plough layer to 0.15 m of brown-grey colour and silty clay loam field texture (MQ–D1); to a structureless light-grey coloured soil with silt loam field texture to 0.4 m (MQ–D2); to a moderately structured, iron mottled (yellow) soil with a light clay field texture (MQ–D3). It was assumed that at greater depths the underlying soil would take on more attributes of a basaltic soil for example, increased structure, iron colouring and clay content.

The nearby paired site was also situated on this southerly facing, gentle slope but was marginally higher up and closer to the nearby road where the effects of cultivation were thought to be minimal. A soil pit was dug to 0.8 m to reveal a very mixed profile dominated by a reddish-brown topsoil to 0.15 m and a banded red-coloured clayey subsoil. Two samples were taken; from the top soil which

evidently had a light clay field texture (MQ–B1), and from the subsoil that also had a light clay field texture (MQ–B2).

Laboratory analyses

For this study, all collected soil samples were subjected to granulometric and mineralogical analysis in the laboratory.

Granulometric analyses

Initially, the particle-size distribution of each of the 14 samples was determined by the pipette method (Gee and Bauder 1986) for material < 20 μm, and wet sieving for material > 53 μm following dispersion in sodium hexametaphosphate. The quantified particle-size fractions were: < 2 μm, 2–20 μm, 20–53 μm, and >53 μm.

As a means of assessing the micro-aggregation of collected soils, particularly the basaltic soils, which often exhibit sub-plastic properties (Norrish and Tiller 1976), the particle-size distribution of all samples were re-assessed using the same size fractions after ultrasonic agitation with a Hielscher UP100H ultrasonic probe (Ultrasound Technology, Inc).

Additionally, the non-clay fraction (2–200 μm) of all samples were analysed using a Coulter Multisizer 3 (Beckman Instruments, Inc). Multisizer analysis produces very high resolution particle-size distributions that encompass 256 size classes per sample (McTainsh *et al.* 1997).

Mineralogical analyses

Five grams of each soil sample (bulk soil) was gently ground to < 53 μm for the determination of the whole mineral suite using a MMA X-Ray Diffractometer (GBC Scientific Equipment, Inc). The dominant minerals were identified using mineral basal spacings as described by Brown (1980).

X-Ray diffraction analysis was also carried out on random powders of the 20–100 μm fraction (‘dust sized’ fraction) of each sample.

Additionally, random powders of two basalt rocks collected during soil sampling were subjected to X-ray diffraction analysis. These rocks are representative of separate Tertiary lava flows in the Mt Canobolas (Pogson and Watkins 1988). The first was collected from Cudal (33°17'25"S, 148°45'19"E) situated on the lower lying, flat region to the north-west of Mt Canobolas, while the other was collected from Huntley (33°23'30"S, 149°6'55"E) which is situated on the extensive lava plain area to the east-south-east of Mt Canobolas .

Micromorphological analyses

Thin sections of undisturbed soil taken from the suspected dust-affected Caldwell soil profile were prepared using soil collected in Kubiëna tins (160 × 80 × 50 mm). The first sample was extracted from the grey silty loam horizon (BD-D1) while the other undisturbed sample was taken from the red

light-medium clay horizon (BD-D3). The soil was dried in the Kubiëna tins and then impregnated with a polyester resin and left to set. Vertically-orientated thin sections 30 μm thick were produced from the impregnated soil and mounted on glass slides. Optical properties of the thin sections were viewed under both plane-polarised light and cross-polarised light using a petrographic microscope and photographed. The micromorphological properties of both thin sections were described using the terminology of Bullock *et al.* (1985).

Modelling loessic soil distribution

Studies reported here use a simple nominal logistic regression approach to define the spatial distribution of loessic material around Mt Canobolas using ancillary sourced information as inputs.

Modelling the spatial distribution of suspected aeolian material was determined across only those areas where basalt rocks are the underlying geologic units. This is because soils derived from this parent material appeared to be clearly distinct from suspected aeolian material in terms of morphological features. This clear distinction could not be assured in areas where soils derived from other parent materials, such as trachytes and rhyolites exist.

Using ArcMap (ESRI ArcGIS 8.2), a 914 km^2 study area encapsulating the Mt Canobolas region was created. This was overlain by merged digital vector files of the Orange and Molong 1:100 000 geological map sheets (NSW Department of Primary Industries, 1997), then clipped to the study area size. All Tertiary basalt units in the study area were extracted to create a new geological map (Fig. 1)**.** This was draped over by a finely resolved (25 m) digital elevation model (DEM) (NSW Department of Lands 2008). Additionally, a number of terrain indices were derived from the DEM and were also draped over the geological map in raster format. Surface terrain indices included; slope, aspect, plan curvature and profile curvature and sediment transport capacity (equivalent to slope length factor in the Revised Universal Soil Loss Equation (Moore *et al.* 1993)). Hydrological indices calculated were flow accumulation potential and flow direction. Secondary terrain attributes included erosive power index and terrain wetness index (function of catchment size and topography). Furthermore, airborne radiometric data in raster format with 50 m ground resolution from the Geophysical Archive Data Delivery System (GADDS) (Geosciences Australia 2008) were acquired and then interpolated onto a 25 m ground-resolution grid and also draped over the geological map.

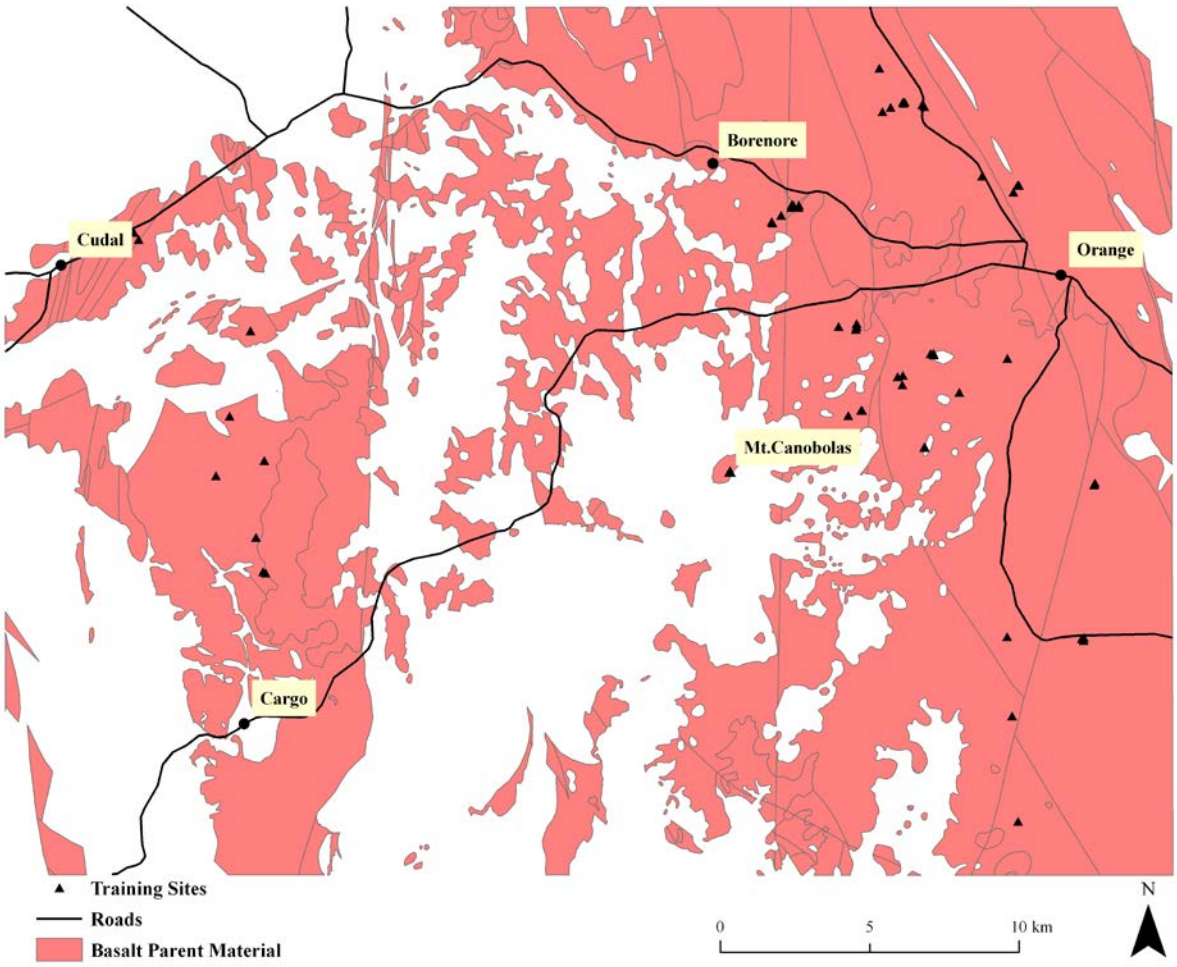

Fig. 1. Locality map of study area and 'training sites' for modelling loessic soil distribution.

To use as inputs for a predictive nominal logistic model, 67 'training sites' scattered throughout the study area (including those at Caldwell, Nashdale, and Towac) were selected to determine whether there was a presence or absence of aeolian material on the soils (Fig. 1). A toposequence sampling regime was adopted to ensure all terrain types in the area were represented. At each training site, a small soil pit was excavated and the top 0.4 m of the profile was examined and sampled for structure, colour and field texture. A topsoil was considered loessic if it was a grey-brown colour with no apparent structure and had an obvious silty texture.

The spatial location of each training site was recorded and coupled with whether there was a presence or absence of suspected aeolian material. This information was brought into ArcMap where it was spatially joined (nearest neighbour method) to the table containing the geo-database containing the elevation, terrain and radiometric data. The resulting table was brought into JMP statistical program (SAS) where a nominal logistic model was created using the elevation, terrain and radiometric data as predictor variables. The model formula was then used to predict the presence or absence of aeolian material for the entire coverage of the study area. A subsequent map of predicted loess distribution was created.

Results

Granulometric features

The particle-size fractions of the soils dispersed with sodium hexametaphosphate (Table 1) show that the clay content fraction (< 2 μm) is lowest in the topsoils of the 'loessic' profiles at each of the three sites. For the BD-D1, LC-D1 and MQ-D1 horizons, the clay-sized fraction did not exceed 6 %, while in the MQ-D2 horizon, the clay fraction was also below 5%. However, for each of these horizons the total silt-sized fraction (2–53 μm) constituted for approximately 64 %, 73 %, 75 % and 69 % of the total fine-earth fraction respectively.

At the 'loessic' sites (BD-D.., LC-D.., MQ-D..), clay content sharply increased with depth with an average of 20% increase in clay between topsoils and subsoils. At Caldwell, clay increased from 22% between 0.2–0.45 m to 58% between 0.45–0.8 m. This trend was not the same at all sites where at Towac with a comparable depth of between 0.4–0.75 m, clay only accounted for 26 % of the total fine earth fraction and the silt-sized fraction accounted for about 53% of the total. The sub-soils of the other 'loessic' sites also had prominent silt-sized fractions, but considerably lower than their topsoil soil counterparts.

The topsoils of the 'basaltic' soil profiles (BD-B.., LC-B.., MQ-B..) were texturally distinct from the nearby 'loessic' profiles. Clay content ranged from 14% in the LC-B1 horizon to 29% in the MQ-B1 horizon. The silt-sized fractions of all 'basaltic' soils ranged between 40–55%.

Table 1. Particle-size fractions as a percentage of the total fine-earth fraction where sodium hexametaphosphate was used as a soil dispersant

Sample	Depth (m)	Sodium hexametaphosphate dispersion			Ultrasonic dispersion		
		< 2μm	2–53μm	> 53 μm	< 2 μm	2–53μm	> 53 μm
BD-D1	0–0.2	5	64	31	9	84	7
BD-D2	0.2–0.45	22	51	27	21	74	4
BD-D3	0.45–0.8	58	31	10	55	43	2
BD-B1	0–0.1	16	58	26	16	76	7
BD-B2	0.4–0.5	42	41	17	41	55	4
LC-D1	0–0.15	6	73	21	6	83	11
LC-D2	0.4–0.5	36	46	17	34	62	4
LC-B1	0–0.1	15	56	29	20	74	6
LC-B2	0.4–0.5	40	43	17	38	58	4
MQ-D1	0–0.15	3	75	22	8	85	7

MQ-D2	0.15–0.4	4	69	26	6	88	5
MQ-D3	0.4–0.75	26	53	20	26	69	4
MQ-B1	0–0.15	29	55	15	35	62	3
MQ-B2	0.6–0.8	35	51	15	35	61	4

Dispersing the soils with ultrasonic agitation had a significant impact on the particle-size distributions of all samples. In particular, coarse-silt fractions (20–53 μm) of all samples were between 13–30% greater after ultrasonic agitation than after using sodium hexametaphosphate as a soil dispersant. Consequently, in the topsoils of 'loessic' profiles, the silt-sized fraction constituted for between 73–88% of the fine earth fraction. In the 'basaltic' soils, the silt-sized fraction accounted for between 55–76% of the total fine earth in these soils. The increase in the overall silt-sized fraction of all soils was found to be countered by an overall decrease in the >53 μm fraction.

The effect that the method of dispersion had on clay content was varied. For horizons such as BD-D1, LC-D1, MQ-D1, LC-B1 and MQ-B1 there was an increase of between 2–5% for the clay-sized fraction in. In other horizons, there was little difference in clay content when comparing both methods of dispersion.

High-resolution particle-size distributions (PSDs) of the ultrasonified samples from Caldwell (Fig. 4) indicate differences in particle-size distribution both within and between the 'loessic' and 'basaltic' profiles. For the 'loessic' profile, both BD-D1 (Fig. 4a) and BD-D2 (Fig. 4b) have a smoothly shaped, uni-modal PSD. The majority of particles range between 22–62 μm and have modal size of 42 μm. Both these samples have < 9% of particles less than 10 μm, while 90% of particles are < 54 μm. However, for the BD-D3 horizon (Fig. 4c), 20% of the non-clay fraction is composed of particles less than 10 μm and 90% below 34 μm. The modal size of particles in this horizon is 20 μm. For the 'basaltic' profile at Caldwell, both BD-B1 (Fig. 4d) and BD-B2 (Fig. 4e) display PSDs with numerous peaks but have a modal size of particles measuring 34 and 36 μm respectively. Both horizons have about 12% of their particles less than 10 μm.

At Nashdale the non-clay fraction of the 'loessic' profile (Figs 5a, 5b) displays a modal particle-size of 35 μm in LC-D1 and 29 μm in LC-D2. While similar in terms of modal size, 26% of particles in LC-D2 were < 10 μm, while for BD-D1 only 10% were. For the 'basaltic' horizons, the modal particle size for LC-B1 and LC-B2 were 23 μm and 34 μm respectively (Figs 5c, 5d). The LC-B1 horizon had 30 % of particles < 10 μm, while LC-B2 horizon had a partial bi-modality with peaks at 25 μm and 34 μm and 10% of particles < 10 μm.

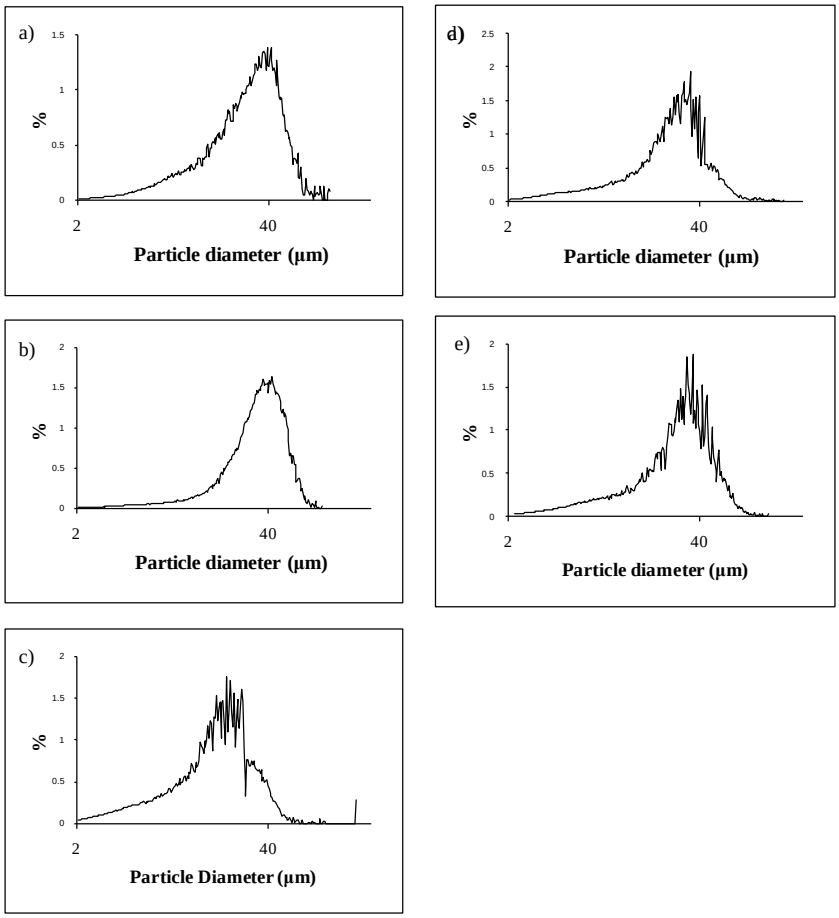

Fig. 4. High-resolution particle-size distributions of Caldwell. (a) BD-D1, (b) BD-D2, (c) BD-D3, (d) BD-B1, (e) BD-B2

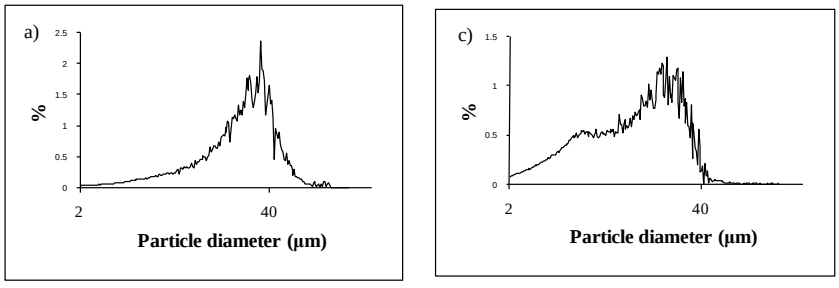

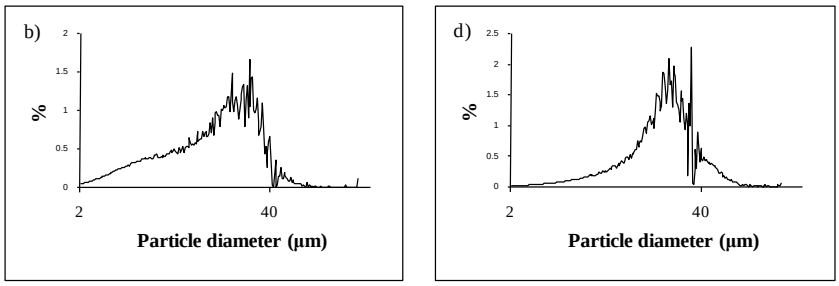

Fig. 5. High-resolution particle-size distributions of Nashdale. (a) LC-D1, (b) LC-D2, (c) LC-B1, (d) LC-B2

The three horizons of the 'loessic' profile at Towac all display a smoothly shaped PSD and had a modal size of particles between 36–39 µm (Figs 6a, 6b, 6c.). In comparison with the other loessic horizons, MQ-D1 had considerably more coarse material but had 90% of particles < 58 µm. In the MQ-D2 and MQ-D3 horizons, 90% of particles were < 45 µm. For all 'loessic' samples, < 15% of particles were less than 10 µm. For the 'basaltic' horizons (Figs. 6d, 6e) both MQ-B1 and MQ-B2 had a modal particle-size of 30 µm and had approximately 25% of all particles < 10 µm.

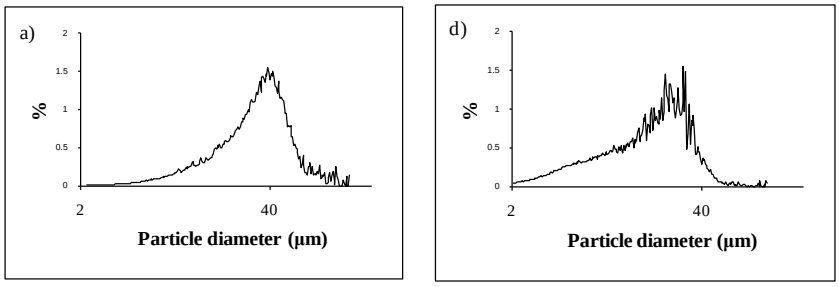

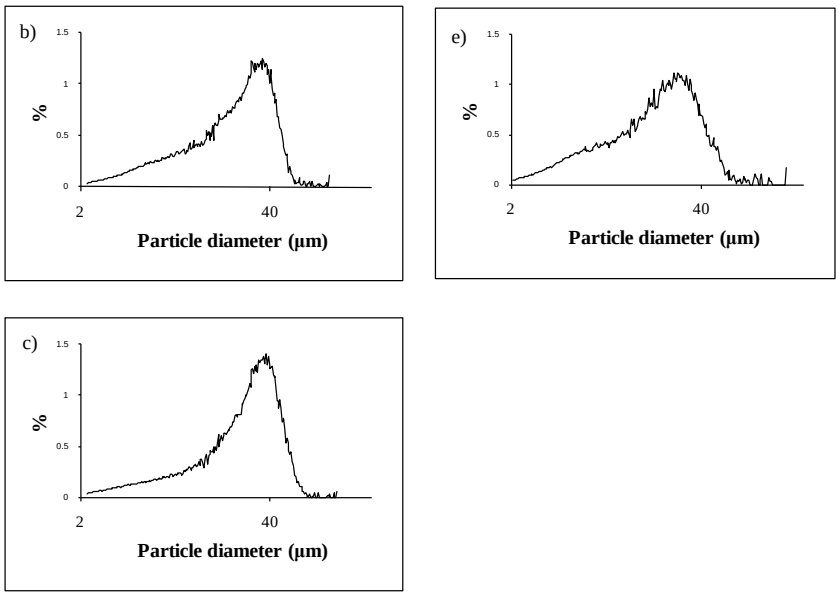

Fig. 6. High-resolution particle-size distributions of Towac. (a) MQ-D1, (b) MQ-D2, (c) MQ-D3, (d) MQ-B1, (e) MQ-B2

Mineralogical features

The minerals that were detected in the bulk soil fractions are summarised in Table 2. The X-ray diffraction results indicate that the 'loessic' profiles at the three sites are enriched with quartz. The topsoils also contain, K-feldspar, plagioclase feldspars, hematite and brookite, and kaolin is a relatively minor mineral. In the subsoils, kaolin was dominant. K-feldspars were also detected at both subsoil depths at Towac, as well as at Caldwell except its dominance decreased with increasing depth. At Nashdale, K-feldspars were not detected in the subsoils.

For the 'basaltic' profiles, quartz enrichment was also apparent. Kaolin was found to be a dominant mineral for both top and subsoils at all three sites, while a range of other minerals including plagioclase feldspars, hematite and brookite were also present. K-feldspars were detected in the topsoils at Caldwell and Nashdale only, and were absent in the Towac basalt-derived soils.

Table 2. Dominant and subdominant minerals detected in the bulk soil (bs) and 'dust-sized' fractions (ds) from Caldwell, Nashdale, and Towac. Quartz (Qz), k-feldspar (Kf), plagioclase feldspar (Pf), hematite (Ht), kaolin (Kn), brookite (Bk), olivine (Ol), magnetite (Mt), ilmenite (It). Mineral dominant (*d*) and mineral sub-dominant (*s*).

Sample	Qz		Kf		Pf		Ht		Kn		Bk		Ol		Mt		It	
	bs	**ds**	**bs**	**ds**	**bs**	**ds**	**bs**	**ds**	**bs**	**ds**	**bs**	**ds**	**bs**	**ds**	**bs**	**ds**	**bs**	**ds**
BD-D1	***d***	***d***	***d***	***d***	***d***	***d***	***d***	***s***	***s***		***d***							
BD-D2	***d***	***d***	***s***	***d***	***d***	***d***	***d***	***s***	***d***									

BD-D3	***d***	***d***			***s***	***d***	***d***	***s***	***d***							
BD-B1	***d***	***d***	***s***	***s***	***d***	***d***	***d***	***d***	***d***	***s***		***d***				
BD-B2	***d***	***d***			***d***	***d***	***d***	***d***	***d***							
LC-D1	***d***	***d***	***d***	***d***		***d***	***d***	***s***	***s***			***s***				
LC-D2	***d***	***d***		***d***	***s***		***d***	***s***	***d***			***s***				
LC-B1	***d***	***d***	***s***	***d***	***s***		***d***	***s***	***d***		***d***	***s***				
LC-B2	***d***	***d***		***d***	***d***	***s***	***d***	***s***	***d***	***s***	***s***					
MQ-D1	***d***	***d***	***d***	***d***	***d***	***d***	***d***	***s***	***s***							
MQ-D2	***d***	***d***	***d***	***d***	***s***	***s***	***d***	***s***	***s***	***s***						
MQ-D3	***d***	***d***	***d***	***s***	***s***	***d***	***d***	***d***	***d***							
MQ-B1	***d***	***d***		***d***	***s***	***d***	***d***	***s***	***d***							
MQ-B2	***d***	***d***		***d***	***s***	***d***	***d***	***s***	***d***	***s***						
Basalt Rocks																
Huntleys						***d***		***s***		***s***				***d***	***d***	***s***
Cudal						***d***		***s***		***s***				***d***	***d***	***s***

The mineral suites of the ‘dust-sized’ fractions of both ‘loessic’ and ‘basaltic’ profiles indicate that there is little to differentiate between the different soil types. The diffractograms indicate that quartz, K-feldspar, hematite and brookite are present in all samples, with the exception of the BD-D3 and BD-B2 horizons where K-feldspar is absent. Plagioclase feldspars were also commonly detected, while olivine was detected only in the BD-B1 and BD-B2 horizons. Kaolin was detected only in minor amounts within the ‘basaltic’ profiles of all sites.

X-ray diffraction of the crushed basalt rock samples indicate that the mineral suites of ‘Huntleys’ and ‘Cudal’ are also alike. This could suggest that the baseline mineral suites of the olivine and porphyritic basalts are similar, or that both rock samples are from the same unit. For both rock samples plagioclase feldspars, olivine, and magnetite are dominant minerals. Hematite, kaolin, ilmenite and psilomelane detected as subdominant minerals in both samples.

Micromorphological features

The topsoil (BD-D1) of the ‘Caldwell loessic’ profile consists predominantly of well-sorted mineral grains ranging between 35–42 μm (Fig. 7a). There is also a combination of coarse and fine organic material distributed unevenly throughout this soil. The mineral skeleton grains vary in shape from angular to sub-rounded and are in a chitonic related distribution, where the grains are linked by braces of fine organic material. Depending on the

concentration of fine material, the structure is a combination of bridged-grain where the grains are partially surrounded and bridged by fine organic material and debris, and massive, where there are few if any discrete voids (Figs 7b, 7e).

The presence of angular and sub-rounded mineral grains measuring between 35–42 μm in diameter can also be seen in the thin-section of BD-D3 (Figs 7c, 7d). The mineral grains are in a porphyric related distribution where they are embedded in a dense clay matrix. The microstructure of this horizon is a combination of granular and chamber. For granular structure (Fig. 7c), granules are separated by compound packing voids and do not accommodate each other. The granules contain few voids or recognisable smaller structural units. Where chamber structure is evident, there are no discrete aggregates and the dominant voids are chambers. Occasionally the edges of these chambers display infillings of clay or clay plugs (Fig. 7d).

Bio-turbation is likely to be an active process in this profile. This is exemplified by the presence of worm castings in the BD-D1 (Fig. 7e). Evidence of topsoil and subsoil mixing is seen in BD-D3 (Fig. 7f) where quartz grains are in both chitonic and porphyric related distributions in the same field of view.

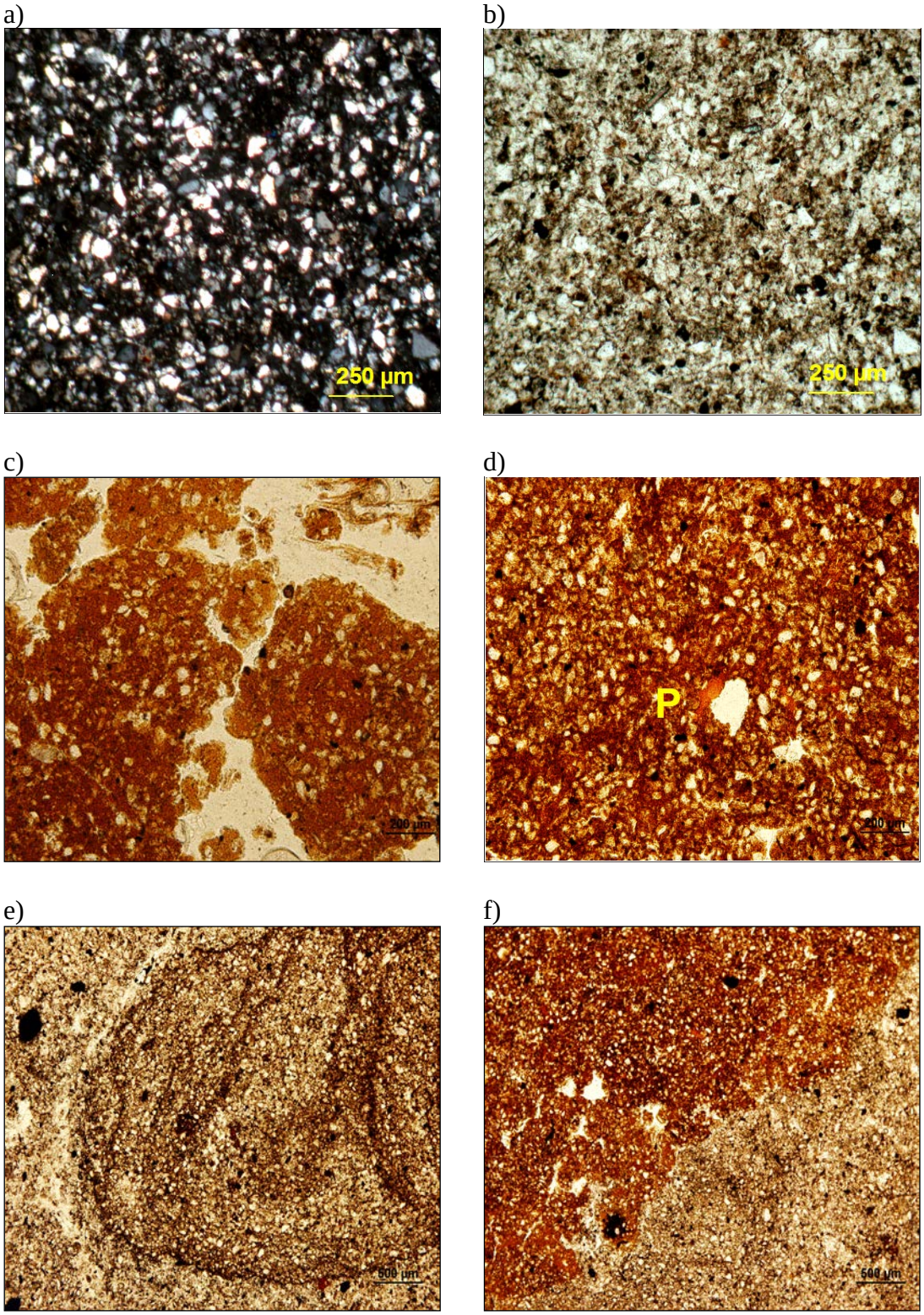

Fig. 7. Photomicrographs of soil thin-sections from Caldwell loessic profile (BD-D1 and BD_D3) (PPL, plane polarised light, XPL, cross polarised light): (a) well-sorted particles showing dominant quartz grain that vary between angular and sub-rounded in shape in BD-D1 (XPL) (b) well-sorted particles in a chitonic fabric from BD-D1 (PPL), (c) well-sorted particles in a porphyric fabric of BD-D3 also showing granular microstructure (PPL) , (d) porphyric fabric and some chamber infillings of clay (P) of BDD3 (PPL), (e) worm castings within BD-D1 (PPL), (f) contrasting porphyric and chitonic fabrics in BD-D3 (PPL)

Modelling the spatial distribution of loessic topsoils

Of the 67 ‘training sites’ used to model the spatial distribution of loessic soils around Mt Canobolas, 13 were sites where there was a prominent topsoil of loessic material. The predictive accuracy of the loessic soil distribution model was assessed by comparing results from the ‘training sites’ with the modelled predictions at each of these sites. The overall accuracy of the model was 81%. However, 38% of actual ‘loessic’ sites were correctly predicted (producer’s accuracy), while 92% of ‘basaltic’ sites were correctly predicted. Of the nine predicted sites that were modelled as being ‘loessic’, five of them (56%) were actual loessic sites (user’s accuracy). The user’s accuracy for ‘basaltic’ sites was 86%. A kappa statistic of 0.35 indicates that there is a fair agreement between actual and modelled predictions.

The subsequent map of the modelled spatial distribution of loessic topsoils in the Mt Canobolas area (Fig. 8) predicts that the silty material is more commonly found on the eastern margins of the area rather than on the western margins. The model estimates that some prominent patches of loessic material are concentrated to the south and northwest of the township of Borenore. There are also some concentrated patches of loessic material in the south western part of the study area and to the south of Mt Canobolas. In other locations, the narrow and long lines of predicted loess material that are distributed randomly throughout the study area appear to follow the meandering nature of watercourse lines. In total about 10% of the area that is underlain by Tertiary basalt rocks is predicted to have at least some of its topsoil composed of loessic material.

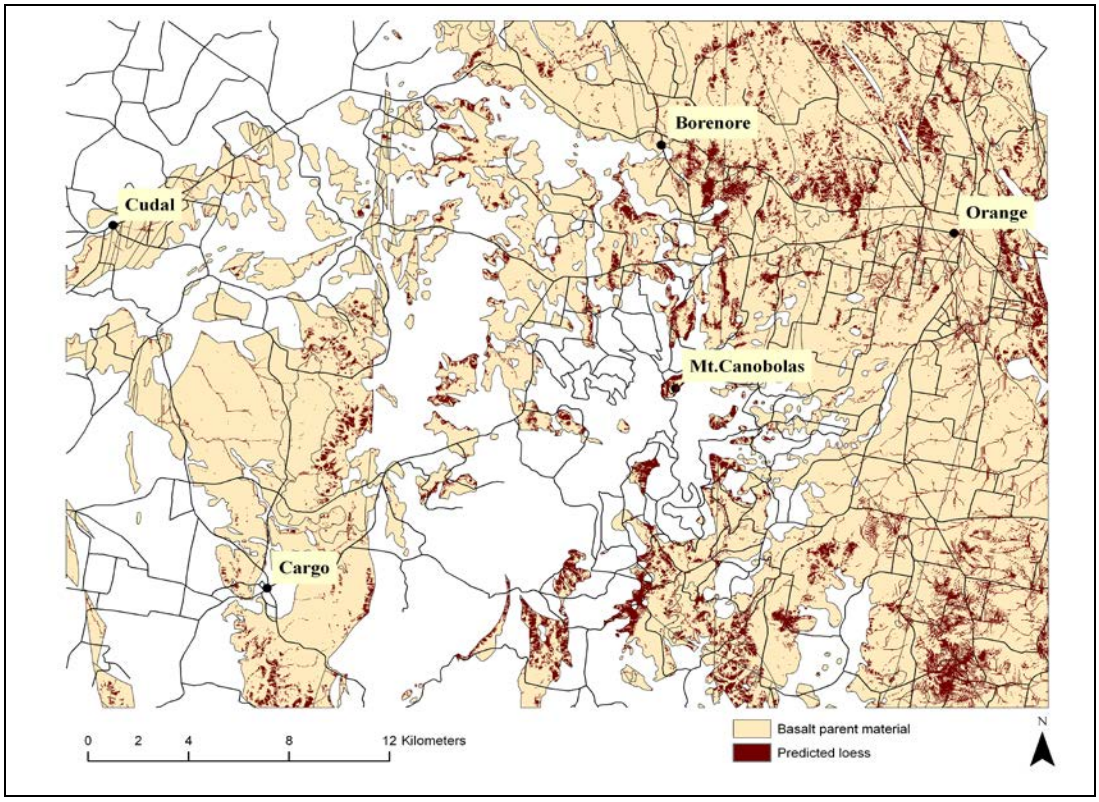

Fig. 8. Map of the Mt Canobolas area displaying the modelled predictions for the spatial distribution of loessic topsoils (coloured maroon) upon *in situ* soils derived from Tertiary basalt rocks

Characteristic attributes of both 'loessic' and 'basaltic' soils were derived from the various ancillary datasets. Elevation appeared to be a fair discriminator of the presence of loessic material as it was most commonly predicted to occur between 800–1000 m a.s.l. Loessic material was less likely to be predicted below 800 m a.s.l, whereas, basalt-derived soils were commonly predicted to occur below this elevation. Additionally, the model estimated that purely basaltic soils occurred in all manner of sloping terrains, but for the loessic soils, they were predicted to occur on flatter to gently sloping land only. However, given the long negative and positive distribution tails of plan and profile curvature respectively, it is likely that some of these gently sloping sites have an element of convergent flow whereby materials and water flow to a central area in the contour. The localities where loessic material was predicted to occur were characterised as either having low or high values for topographic wetness index values (TWI). In contrast, for soils derived from basalt, they were modelled to not occur in catchment accumulation points (low to medium TWI values) and were found equally distributed between both convergent and divergent landforms.

For the other ancillary variables such as all the radiometric data, and terrain indices including aspect, erosive power, flow accumulation flow direction and sediment transport

capacity, there were no characteristic differences from which to discern between sites that had loessic material and those that did not.

Discussion

Demonstrating an aeolian origin of the 'loessic' topsoil

The results indicate that the textural and morphological properties of the 'loessic' soils contrast significantly to those that have been derived from basalt. When comparing the 'loessic' topsoils with the 'basaltic' soils, it is clear there is a significant colour difference between the two materials. The 'loessic' material is a grey colour and contrasts remarkably to that of the orange-red colour of the 'basaltic' soil, indicating distinctly different abundances of free-iron oxide minerals. Additionally, the 'loessic' material displays a massive, loose grain packing structure found to be common in aeolian derived soils (Pye, 1995), which is distinct from the strong granular structure with large compound packing voids found for the 'basaltic' soils.

Characteristic textural features of the 'loessic' materials included negligible clay content and a significant abundance of silt-sized particles. In comparison, the 'basaltic' soils also contained an abundance of silt-sized particles, albeit less of a proportion of the fine-earth fraction, but are considerably more clay-rich than the 'loessic' soils. The characteristic 'dust-sized' particle features of both the 'loessic' and 'basaltic' are contrasted enough to indicate they are both not of the same derivation. For the 'basaltic' soil profiles at each of the three study locations, the 'dust-sized' particle-size distribution was not well-sorted and their modal size was always consistently < 35 μm. It is rare that *in situ* soils and sediments display a well-sorted population of particles with clear modality (McTainsh and Hesse, 2003). In contrast, the 'loessic' materials contained a significant abundance of silt-sized particles that consistently ranged in size between 35–42 μm. This conspicuous population of well-sorted particles signifies that the material is aeolian, where such particles can easily be entrained by wind during dust storms. Previous aeolian dust research in eastern Australia have interpreted that the presence of a particle-size mode in the 30–60 μm range is indicative of aeolian dust accession (Beattie 1970; Cattle *et al.* 2002; Humphreys *et al.* 2002; Tate *et al.* 2007).

It is unknown as to the full extent of micro-aggregation in both the 'loessic' or 'basaltic' soils when comparing the coarse-silt populations following each of the two different methods of dispersion. The significant increase in coarse-silt particles and a decrease in fine sand particles following ultrasonic dispersion indicate that regardless of soil type, various binding agents are micro-aggregating soil particles together. Common cementing or particle binding

agents include organic matter and iron and aluminium oxides (Goldberg *et al.* 1990) and have been widely regarded as responsible for the incomplete dispersion of soils (Norrish and Tiller, 1976). Considering that the 'loessic' soils contain appreciable amounts of organic matter, and the 'basaltic' soils are rich in iron oxides, it is possible that both these soil types display some sub-plastic properties. However, this raises the question of whether ultrasonification was suitable considering that clay fractions, particularly in the 'basaltic' soils remained virtually unchanged. It could be that for all samples, there was enough energy the disperse the aggregated fine sand particles, but not enough to disperse any of the smaller aggregated particles that could have existed as more energy was required to do this. Micromorphological evidence indicates that it is unlikely for the 'loessic' soils to display any more micro-aggregating features than they already have. However, for the 'basaltic' soils, it is possible that further ultrasonification could yield higher clay content for these soil types, but on the other hand, the lighter textures of these soils may be due to the enrichment of quartz particles that were abundantly detected in these soils.

The mineralogical characteristics of both basalt rocks confirm that the 'basaltic' soils have been derived from them, whereby the rocks contained appreciable amounts of plagioclase feldspars that were also detected in the soils. The basalt-derived soils also contained a significant amount of the secondary clay mineral kaolin as well as iron oxide minerals, which was to be expected when considering the weatherability of primary minerals including olivine found in abundance in the basalt rock. The fact that some kaolin was detected in minor quantities in the crushed rock samples typifies the weathering process of these basalt rocks.

It could be argued that because quartz and K-feldspar were detected in the 'basaltic' soils, the 'loessic' material could also have been derived from a basalt parent material. Although not a natural phenomenon due to the fast cooling time of basalt magma, it is not uncommon for basalt rocks to contain some quartz (Raymond 2002). Baldridge *et al.* (1996) discuss some of the likely events that contribute to the existence of quartz-bearing basalts that include quartz entrainment in basalt magma through contamination by, and partial digestion of, quartz-bearing crustal rocks. Considering that much of the Mt Canobolas area is underlain by quartz-bearing granitoids (Pogson and Watkins 1998), this explanation seems warranted. However, XRD of the rock samples failed to detect any sign of quartz and therefore points to other possible sources. This could include the quartz-bearing trachytes and rhyolites that are extensive in the area. Sediments derived from these rocks could have been mobilised by water or wind processes and deposited upon the basaltic soils, where over time, various soil-

mixing processes have incorporated these materials. However, the first process of this scenario is unlikely at sites such as Caldwell and Nashdale where additions of water-borne sediment are not possible. Furthermore, while, it is suspected that this material has an aeolian origin, the particle size features of the quartz (modal size of between 35–42 μm) if aeolian are too fine for the material to have been locally sourced. Tsoar and Pye (1987) estimate that the modal particle-size of locally derived dust deposits measure > 50 μm. Therefore, given the fact that the quartz particles in both 'loessic' and 'basaltic' soil types are well sorted and of comparable size, the likely scenario is that the quartz has been derived from the 'loessic' material. For the soil profiles that have been regarded as being wholly basalt-derived, it is likely that these could have been sites where the 'loessic' material has not been preserved, which has since washed away. Over time, soil mixing via cultivation and bio-turbation processes have incorporated the leftover residual material into the subsoils. This is the same scenario for the occurrence and incorporation of K-feldspar in the 'basaltic' soils. Firstly, this is because basalt rocks contain very little elemental potassium. Additionally, the measured particle-size characteristics do not correlate with those for locally-derived dusts. Nevertheless, it is likely that feldspars are less abundant than quartz in the 'loessic' material.

In terms of mineralogical composition, loess soils can be mineralogically diverse due the varied nature of their source (Pye 1987) and thus it is difficult to prescribe a mineralogical signature for aeolian dust deposits. Nevertheless, besides quartz, commonly found minerals in Australian dust deposits have included feldspar, calcium carbonate and clay minerals such as kaolin and illite (Hesse and McTainsh 2003). Dickson and Scott (1998) reported the presence of K-feldspar, plagioclase, hematite, muscovite, kaolin and anatase when they characterised loessic soils around Blayney on the NSW Central Tablelands. For this study, 'dust-sized' quartz and K-feldspars were found to be allochthonous minerals and therefore are one of the diagnostic features of dust deposits in the Mt Canobolas area. The loessic material may also contain hematite, plagioclase, brookite and kaolin. However, this is uncertain because of their presence also in the basalt-derived soil materials

In other evidence, the presence of sub-rounded quartz grains observed in the 'loessic' soil thin-section could be interpreted as being characteristic of an aeolian dust material. While a matter of conjecture, Pettijohn *et al.* (1987) suggest that grain rounding is a slow process and requires significant periods of fluvial or aeolian activity to effect changes in the originally angular quartz grains. In addition to this, Krinsley and McCoy (1978) state that for aeolian dusts, grain rounding occurs in suspension when there are frequent collisions between individual grains. Furthermore, previous studies have reported rounded to sub-rounded quartz

grains as a characteristic of aeolian dusts (Stanley and De Dekker 2002; Hesse *et al.* 2003). However, Pye and Sherwin (1999) stipulate that in addition to pre-depositional weathering while in suspension, the shape of dust grains are also a reflection of mineral composition, mode of formation, and the degree of post-depositional modification induced by weathering. Therefore, as Ryan and Cattle (2006) argued after observing aeolian grains from the same-deposited material that had a combination of angular and sub-rounded shapes, grain morphology may not necessarily be a useful diagnostic attribute of aeolian dust.

The source of the aeolian material

The appreciable distance between sites where the 'loessic' material has been identified; their similarity in composition; and their existence as massively structured discrete units upon lithologically distinct soils and parent materials indicates that the 'loessic' material has been transported into the area via aeolian processes. Similar criteria have also been used previously to indicate aeolian processes in south eastern Australia (Butler 1956; Beattie 1970; Chen 1997; Humphreys *et al.* 2002). The defining feature of the loessic soils around Mt Canobolas is their consistent particle size of between 35–42 μm. According to Tsoar and Pye (1987) who grouped dust deposit PSDs into transport categories based on the predominant size mode, it is likely that the aeolian material around Mt Canobolas has been regionally sourced. This source area could be from anywhere from tens to a thousand or more kilometres away. In south eastern Australia, Bowler (1976) identified that present and past dust-raising winds relate to easterly moving frontal systems across the continent. Furthermore, Dickson and Scott (1998) pointed out that for the Central West of NSW, winds carrying dust are generally westerlies or hot northerlies, blowing from Central Australia and preceding frontal systems. Considering the well-sorted particles found in the loess soils around Mt Canobolas area, these dry summer northerlies and westerlies supports the notion that the mode of dust deposition is that of dry deposition, where particles settle out of suspended transport in accordance with their mass (Cattle *et al.* 2008). It is therefore likely that trachyte or other quartzose and/or felsic provinces in the central west or western NSW (Raymond *et al.* 2000) are the possible sources of the aeolian deposits around the Mt Canobolas area.

Given the granulometric and mineralogical characteristics of these aeolian dust deposits, it is clear they differ significantly from the clayey, calcareous 'parna' soils in southern NSW as described by Butler (1956). Instead, the 'loessic' material is more similar in composition to that of the silty 'loess' situated on the Loess Plateau in north western China (Pye 1987). They

are also less clayey and slightly coarser textured in terms of the modal particle-size, than the loess mantles characterised by Humphreys *et al.* (2002) around Blayney, NSW.

The distribution of loessic soils around Mt Canobolas

Walker and Costin (1971) proposed that hills in the path of oncoming winds create areas of lower wind velocity on the leeward side, which causes an increase in the deposition of dust in undulating landscapes. It is therefore possible that because of major uplifting in the landscape around Mt Canobolas, there have been significant amounts of dust deposited over the course of time. The modelled distribution of loessic soil around Mt Canobolas is representative of this process whereby dust deposition was minimal in the western section (windward) of the study area, relative to the eastern section (leeward). In the west, around the townships of Cudal and Cargo, the terrain is flatter and situated lower in the landscape. However, heading east from this area, the terrain becomes significantly more uplifted and complex in topography. Consistent with the dominant dust carrying northerlies and westerlies (Dickson and Scott 1998), it would appear that this uplifted terrain has acted as a significant barrier in the path of suspended dust.

There is no evidence the aeolian material around Mt Canobolas blankets the landscape like 'parna' does throughout southern NSW (Chen 2001). Conversely, it appears to exist in two separate forms, the first of which is in discrete patches as a thin layer on the crests of gentle slopes, mantling the underlying basalt-derived soils. The predictive model characterises these sites as been situated at the top of a catchment point (Low TWI) where water-borne sediment is unlikely to build up. It is likely that these sites are primary sites of dust deposition, which are exemplified at both Caldwell and Nashdale.

The other form in which the loess is predicted to exist in the Mt Canobolas area is as a thick deposit in topographic depressions and presumably upon the *in situ* derived soils. The accumulation of loess in valley bottoms and topographic depression is not uncommon, particularly in steep terrain and poorly vegetated areas (Pye 1995). Given the poor structural characteristics of the loessic material and its negligible cohesive strength, the accumulation of loessic material in topographic depressions indicates the aeolian material is easily mobilised by erosive forces and then re-deposited in sites of secondary dust deposition i.e. catchment-accumulating areas. It appears these particular deposits exist within convergent landforms and are characterised as having a high TWI value and therefore almost certainly susceptible to colluvial enrichment of water-borne sediment. The thick profile of loessic material

observed at Towac exemplifies this particular form of loess deposition as it is situated in a lower lying area, flanked by gentle to medium-sloped hills in all directions.

Besides elevation and the nature of sloping land as being useful predictors of dust accumulation around Mt Canobolas, other terrain and hydrological indices did not appear useful for discerning loessic soil distribution. Besides a need for more training sites, it is likely that factors relating to dust deposition and possible re-mobilisation of this material within the complex landscape could be difficult physical processes to define in a modelled environment. Processes such as erosion and colluvial movement of sediment are equally likely to affect the basalt-derived soils, as they are the loessic soils, making it difficult to differentiate the two. It is also unfortunate that radiometric anomalies between the loessic and 'basaltic' soils could not be defined, considering the higher concentration of K-feldspar in the loessic material as opposed to that upon the topsoils of the 'basaltic' soils. While there has been mixed success in the past with using radiometric survey as a tool for discerning areas of dust accumulation (Cattle *et al.* 2003), it was envisaged that because the loessic soils have a higher abundance of K-feldspar, the gamma-rays of potassium would be higher in the areas where they were situated. However, this discrepancy may signify that the resolution of the radiometric data was too coarse for this application. The ground-resolution of the radiometric data was 50 m. However, from observations at the study locations and various 'training sites' it appeared unlikely that an area of loessic material covered 250 m^2. Therefore, the spectrometer is unlikely to discern slight radiometric anomalies and instead measures the dominant gamma-rays emitted from the surrounding land dominated by basalt-derived soils. In future studies, ground-truthing with a portable gamma-ray spectrometer could be advantageous for determining the true radiometric signature of the loess material.

In consideration of the extensive study area and the small number of 'training sites', which were disproportionately situated where the loessic material did not exist, logistic modelling is a fast and reasonably incisive method for determining the spatial distribution of dust-derived soils. With some modifications, this current predictive framework has the potential to be expanded into other areas where dust deposition is thought to have occurred.

Conclusions

There is compelling evidence that some soils in the Mt Canobolas area have a distinctive aeolian component. These loessic soils differ significantly from the 'parna' soils first described by Butler (1956). In these soils;

- the topsoil material is morphologically distinct from and is considerably less clayey than the underlying *in situ*-derived soil,
- the clay content rarely exceeds 9% of the fine-earth fraction,
- a characteristically well sorted 'dust-sized' particle distribution exists where the modal particle-size is between 35–42 µm,
- the mineral suite is dominated by quartz and K-feldspar which indicates this material is allochthonous, and
- the presence of sub-rounded quartz grains is suggestive this material was once suspended aeolian dust.

The uplifted nature of Mt Canobolas and its surrounding landscape are thought to have acted as a significant barrier in the path of suspended dust that has travelled from tens to a thousand or more kilometres from its source presumably in central western or western NSW.
Subsequent dust deposition has occurred, resulting in the formation of loessic soils that can currently be found throughout the area, particularly at higher elevations either as thin deposits mantling *in situ* derived soils or as thick deposits in topographic depressions.

References

Baldridge WS, Sharp ZD, Reid KD (1996) Quartz-bearing basalts: Oxygen isotopic evidence for crustal contamination of continental mafic rocks. *Geochimica Et Cosmochimica Acta* **60**, 4765–4772.

Barrows TT, Stone JO, Fifield LK, Cresswell RG (2001) Late Pleistocene glaciation of the Kosciuszko Massif, Snowy Mountains, Australia. *Quaternary Research* **55**, 179–189.

Beattie JA (1970) Peculiar features of soil development in Parna deposits in Eastern-Riverina, N,S,W. *Australian Journal of Soil Research* **8**, 145–156.

Bierwirth PN, Brodie RS (2008) Gamma-ray remote sensing of aeolian salt sources in the Murray-Darling Basin, Australia. *Remote Sensing of Environment* **112**, 550–559.

Bowler JM (1976) Aridity in Australia- age, origins and expression in aeolian landforms and sediments. *Earth-Science Reviews* **12**, 279–310.

Brown G (1980) Associated minerals. In 'Crystal Structures of Clay Minerals and their X-Ray Identification'. (Eds GW Brindley, G Brown) pp. 361–411. (Mineralogical Society: London).

Bullock P, Fedoroff N, Jongerius A, Stoops G, Tursina T (1985) 'Handbook for Soil Thin Section Description ' (Waine Research: Albrighton, UK).

Bureau of Meteorology (BOM), (2008). Climate averages. In: (Bureau of Meteorology Website, date accessed: 29/09/08. http://www.bom.gov.au/climate/averages).

Butler BE (1956) Parna-An Aeolian clay. *Australian Journal of Science* **18**, 145–151.

Cattle SR, McTainsh G, Elias S (2008) Aeolian dust deposition rates: particles-sizes and contributions to soils along a transect in semi-arid New South Wales, Australia. *Sedimentology* **In Publication**.

Cattle SR, McTainsh GH, Wagner S (2002) Aeolian dust contributions to soil of the Namoi Valley, northern NSW, Australia. *Catena* **47**, 245–264.

Cattle SR, Meakin SN, Ruszkowski P, Cameron RG (2003) Using radiometric data to identify aeolian dust additions to topsoil of the Hillston district, western NSW. *Australian Journal of Soil Research* **41**, 1439–1456.

Chen XY (1997) Quaternary sedimentation, parna, landforms, and soil landscapes of the Wagga Wagga 1:100 000 map sheet, south-eastern Australia. *Australian Journal of Soil Research* **35**, 643–668.

Chen XY (2001) The red clay mantle in the Wagga Wagga region, New South Wales: evaluation of an aeolian dust deposit (Yarabee Parna) using methods of soil landscape mapping. *Australian Journal of Soil Research* **39**, 61–80.

Dare-Edwards AJ (1984) Aeolian clay deposits of southeastern Australia- parna or loessic clay. *Transactions of the Institute of British Geographers* **9**, 337–344.

Dickson BL, Scott KM (1998) Recognition of aeolian soils of the Blayney district, NSW: implications for mineral exploration. *Journal of Geochemical Exploration* **63**, 237–251.

Gee GW, Bauder JW (1986) Particle-size analysis. In 'Methods of Soil Analysis: Part 1. Physical and Mineralogical Methods'. (Ed. A Klute) pp. 383–411. (American Society of Agronomy, Inc: Madison, WI).

Geosciences Australia, (2008). Radiometric data of the Bathurst 1:250 000 topographic map sheet. In (Geophysical Archive Data Delivery System (GADDS) Website, date accessed 15/05/08.http://www.geoscience.gov.au/bin/mapserv36?map=/public/http/www/geoportal/gadds/gadds).

Goldberg S, Kapoor BS, Rhoades JD (1990) Effect of aluminium and iron oxides and organic matter on flocculation and dispersion of arid zone soils. *Soil Science* **150**, 588–593.

Haberlah D (2007) A call for Australian loess. *Area* **39**, 224–229.

Hesse PP, Humphreys GS, Smith BL, Campbell J, Peterson EK (2003) Age of loess deposits in the Central Tablelands of New South Wales. *Australian Journal of Soil Research* **41**, 1115–1131.

Hesse PP, McTainsh GH (2003) Australian dust deposits: modern processes and the Quaternary record. *Quaternary Science Reviews* **22**, 2007–2035.

Humphreys GS, Hesse PP, Peterson EK, Campbell J, Conaghan PJ (2002) Loess-like deposits at Blayney, south-eastern Australia, Symposium 49 Paper 1987. In '17 th World Soil Congress'. Thailand.

Isbell RF (1996) 'The Australian Soil Classifcation.' (CSIRO Australia: Collingwood, VIC).

Kovac M, Lawrie JA (1990) 'Soil Landscapes of the Bathurst 1:250 000 Sheet.' (Soil Conservation Service of NSW: Sydney).

Krinsley DH, McCoy F (1978) Aeolian quartz sand and silt. In 'Scanning electron microscopy in the study of sediments. A symposium'. (Ed. DH Walley) pp. 249–260. (Geo Abstracts: Norwich).

McTainsh G, Strong C (2007) The role of aeolian dust in ecosystems. *Geomorphology* **89**, 39–54.

McTainsh GH, Lynch AW, Hales R (1997) Particle-size analysis of aeolian dusts, soils and sediments in very small quantities using a coulter multisizer. *Earth Surface Processes and Landforms* **22**, 1207–1216.

Moore ID, Gessler PE, Nielsen GA, Peterson GA (1993) Soil attributes prediction using terrain analysis. *Soil Science Society of America Journal* **57**, 443–452.

Norrish K, Tiller KG (1976) Sub-plasticity in Australian soil. 5. Factors involved and techniques of dispersion

Australian Journal of Soil Research **14**, 273–289.

NSW Department of Primary Industries, (1997). Molong 1:100 000 geological sheet. In (NSW Department of Primary Industries Website, date accessed: 04/06/08. http://www.dpi.nsw.gov.au/minerals/geological/geological-maps/1-100-000).

NSW Department of Primary Industries, (1997). Orange 1:100 000 geological sheet. In (NSW Department of Primary Industries Website, date accessed: 04/06/08. http://www.dpi.nsw.gov.au/minerals/geological/geological-maps/1-100-000).

NSW Department of Lands, (2008). Digital Elevation Data. (NSW Department of Lands: NSW)

Pettijohn FJ, Potter PE, Siever R (1987) 'Sand and sandstone.' (Springer-Verlag: New York).

Pogson DJ, Watkins JJ (1998) 'Bathurst 1:250 000 Geological Map Sheet SI/55-8: Explanatory Notes.' (Geological Survey of New South Wales: Sydney).

Pye K (1987) 'Aeolian dust and dust deposits.' (Academic Press: London, UK).

Pye K (1995) The nature, origin and accumulation of loess *Quaternary Science Reviews* **14**, 653–667.

Pye K, Sherwin D (1999) Loess. In 'Aeolian environments, sediments and landforms'. (Eds AS Goudie, IS Livingstone, S). (John Wiley and Sons Ltd: Chichester, UK).

Raeside JD (1964) Losess deposits of the South Island, New Zealand, and soils formed on them. *New Zealand Journal Geology Geophysics* **7**, 811–838.

Raymond LA (2002) 'Petrology: the study of igneous, sedimentary and metamorphic rocks.' (McGraw Hill: Boston, USA).

Raymond OL, Duggan MB, Lyons P, Scott MM, Sherwin L, Wallace DA, Krynen JP, Young GC, Wyborn D, Glen RA, Percival IG, Leys M (2000) 'Forbes 1:250 000 Geological Sheet SI/55-07: Explainatory Notes.' (Geoscience Australia: Canberra).

Ryan AL, Cattle SR (2006) Do sand dunes of the lower Lachlan floodplain contain the same dust that produced parna? *Australian Journal of Soil Research* **44**, 769–781.

Scott KM (2003) Blayney-Orange District, New South Wales. CRC LEME, CSIRO Exploration and Mining, North Ryde, NSW.

Simonson RW (1995) Airborne dust and its significance to soils. *Geoderma* **65**, 1–43.

Stace HCT, Hubble GD, Brewer R, Northcote KH, Sleeman JR, Mulcahy MJ, Hallsworth EG (1968) 'Handbook of Australian Soils.' (Rellim Technical Publications: Glenside, SA).

Stanley S, De Deckker P (2002) A Holocene record of allochthonous, aeolian mineral grains in an Australian alpine lake; implications for the history of climate change in southeastern Australia. *Journal of Paleolimnology* **27**, 207–219.

Summerell GK, Dowling TI, Richardson DP, Walker J, Lees B (2000) Modelling current parna distribution in a local area. *Australian Journal of Soil Research* **38**, 867–878.

Tate SE, Greene RSB, Scott KM, McQueen KG (2007) Recognition and characterisation of the aeolian component in soils in the Girilambone Region, north western New South Wales, Australia. *Catena* **69**, 122–133.

Tsoar H, Pye K (1987) Dust transport and the question of desert loess formation. *Sedimentology* **34**, 139–153.

Walker PH, Costin AB (1971) Atmospheric dust accession in south-eastern Australia. *Australian Journal of Soil Research* **9**, 1-8.

Appendix 1

Tabular format of geo-referenced points in the Mt Canobolas area, each with unique elevation, terrain and radiometric data values

Point #	Elevation (m)	Potassium (counts/sec)	Thorium (counts/sec)	Uranium (counts/sec)	Aspect (°)	Erosive Power Index	Flow Accumulation (pixels)	Flow Direction (Pixels)	Plan Curvature (co-efficient)	Profile curvature (co-efficient)	Sediment Transport Capacity (slope length factor)	Slope (°)	TWI
1	879	106.3074	25.8446	17.602	261.8699	2.1205	2	8	0	0	0.8434	2.0249	7.5187
2	880	105.5217	26.6757	17.3297	270	1.0805	1	16	0	0	0.5021	1.7184	7.1712
3	881	105.5217	26.6757	17.3297	251.565	0.1908	0	16	0	-0.16	0.1138	0.9059	6.7079
..	..	..	..	..	..	..	..	..	..	..	..	..	..
..	..	..	..	..	..	..	..	..	..	..	..	..	..
..	..	..	..	..	..	..	..	..	..	..	..	..	..
..	..	..	..	..	..	..	..	..	..	..	..	..	..
999042	877	126.9244	24.3727	18.8954	63.4349	10.1817	9	1	-0.112	0.208	2.5457	2.5606	8.6197
999043	876	137.5094	23.7647	19.1336	56.3099	12.5411	14	1	-0.064	0.096	2.4838	2.0649	9.257

Appendix 2

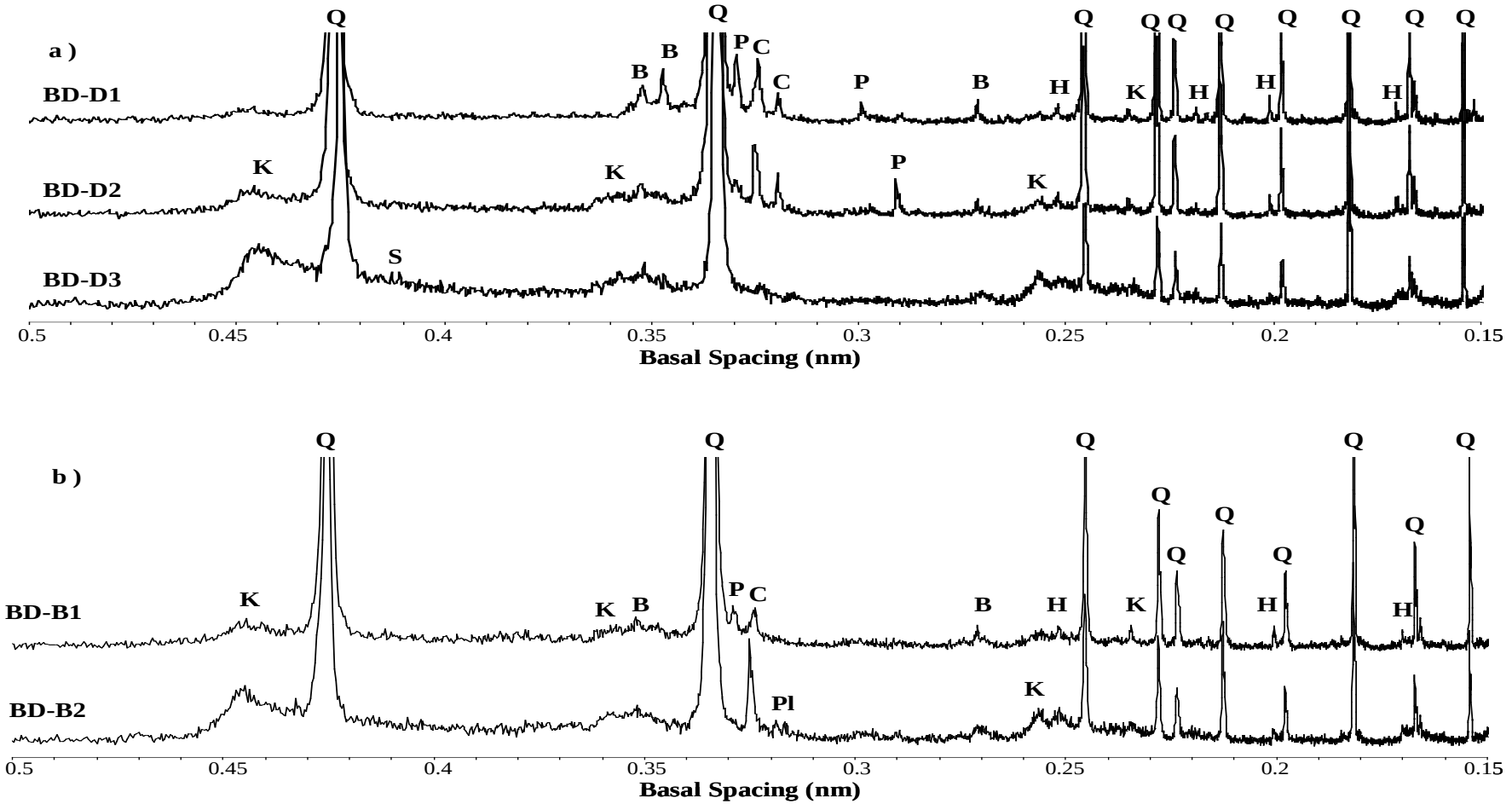

Fig. 1. X-Ray diffractograms of bulk soil from Caldwell (a) Caldwell loessic, (b) Caldwell basalt. (K, Q, B. P, C, Pl, S and H are for kaolin, quartz, brookite, K-feldspar, Ca-feldspar, plagioclase, Na-feldspar and hematite respectively)

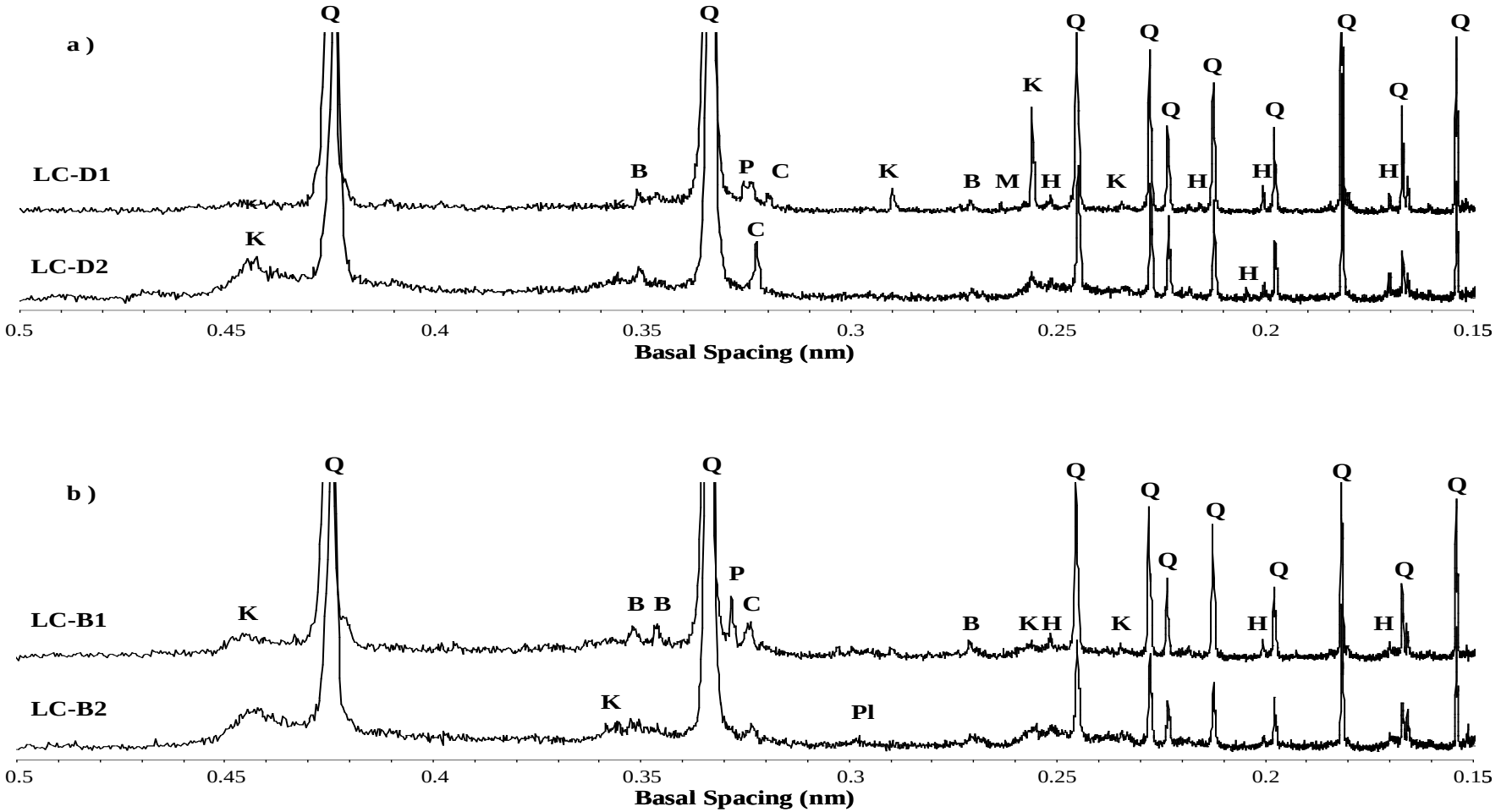

Fig. 2. X-Ray diffractograms of bulk soil from Nashdale. (a) Nashdale loessic, (b) Nashdale basalt. (K, Q, B. P, C, Pl, M and H are for kaolin, quartz, brookite, K-feldspar, Ca-feldspar, plagioclase, magnetite and hematite respectively)

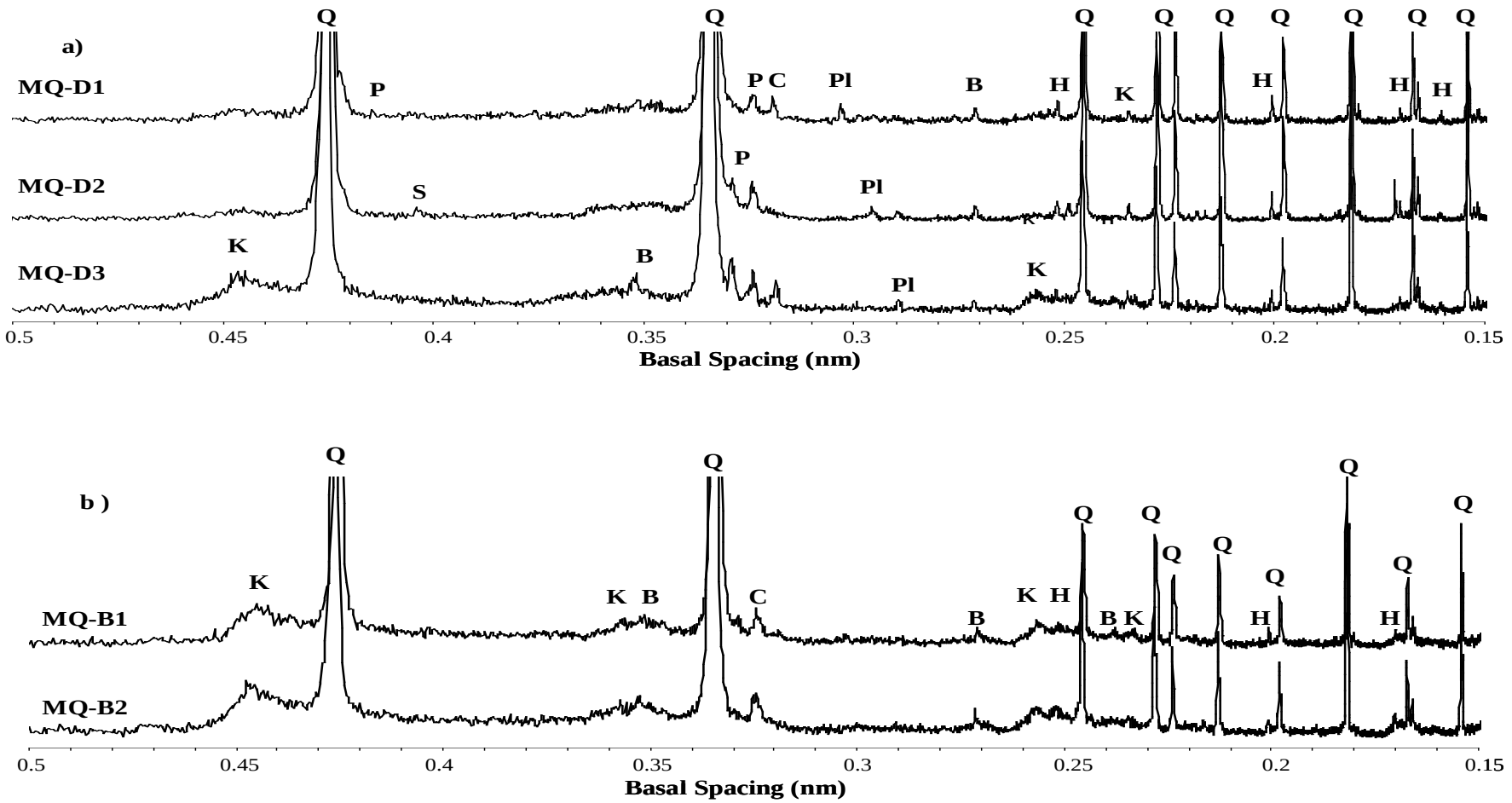

Fig. 3. X-Ray diffractograms of bulk soil from Towac. (a) Towac loessic, (b) Towac basalt. (K, Q, B. P, C, Pl, S and H are for kaolin, quartz, brookite, K-feldspar, Ca-feldspar, plagioclase, Na-feldspar and hematite respectively)

Appendix 3

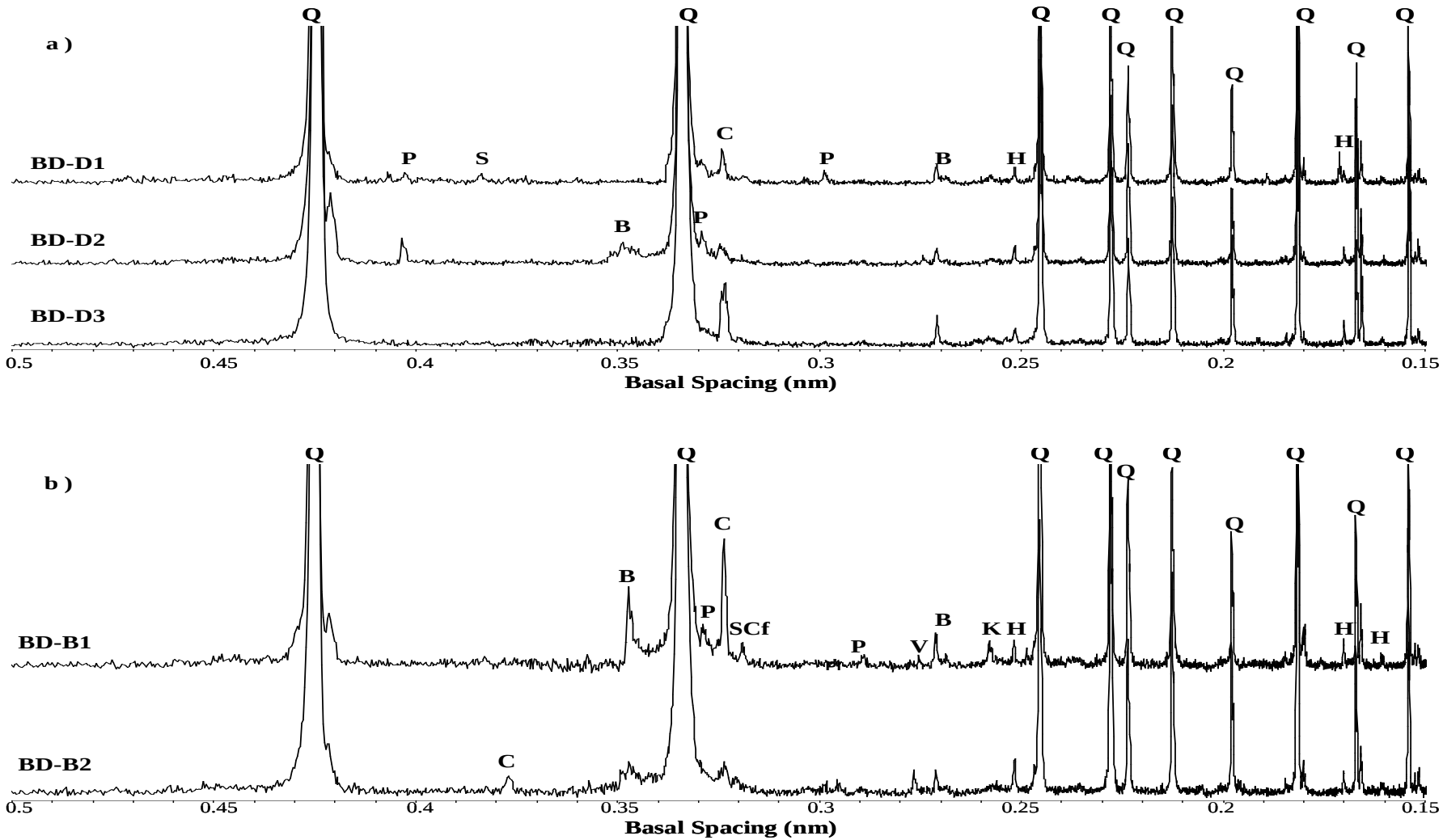

Fig. 1. X-Ray diffractograms of 'dust-sized' fraction from Caldwell. (a) Caldwell loessic, (b) Caldwell basalt. (K, Q, B. P, C, Pl, S, SCf and H are for kaolin, quartz, brookite, K-feldspar, Ca-feldspar, plagioclase, Na-feldspar, Na-Ca-feldspar and hematite respectively)

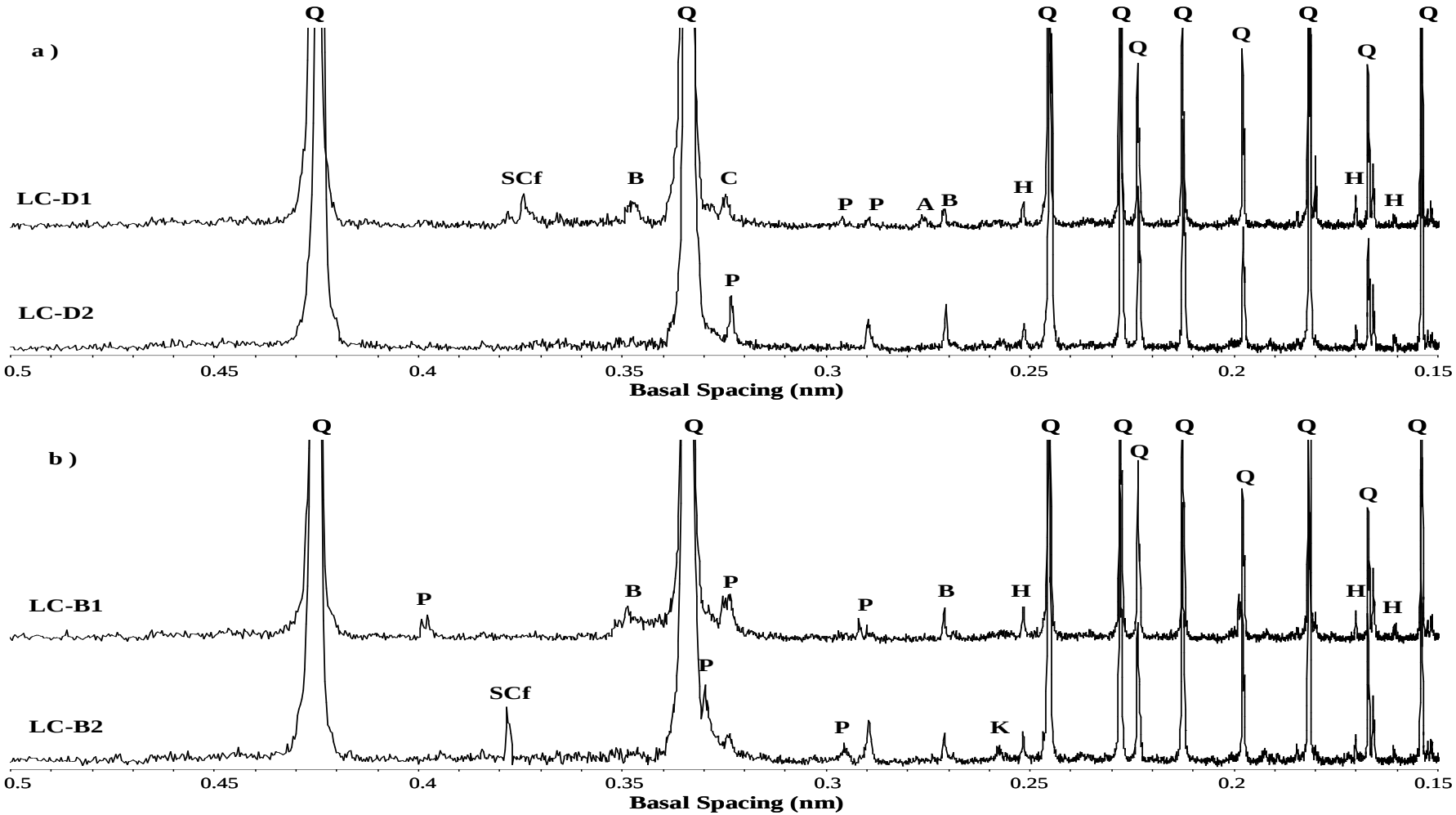

Fig. 2. X-Ray diffractograms of ‘dust-sized’ fraction from Nashdale. (a) Nashdale loessic, (b) Caldwell basalt. K, Q, B. P, C, A, SCf and H are for kaolin, quartz, brookite, K-feldspar, Ca-feldspar, alumina, Na-Ca-feldspar and hematite respectively)

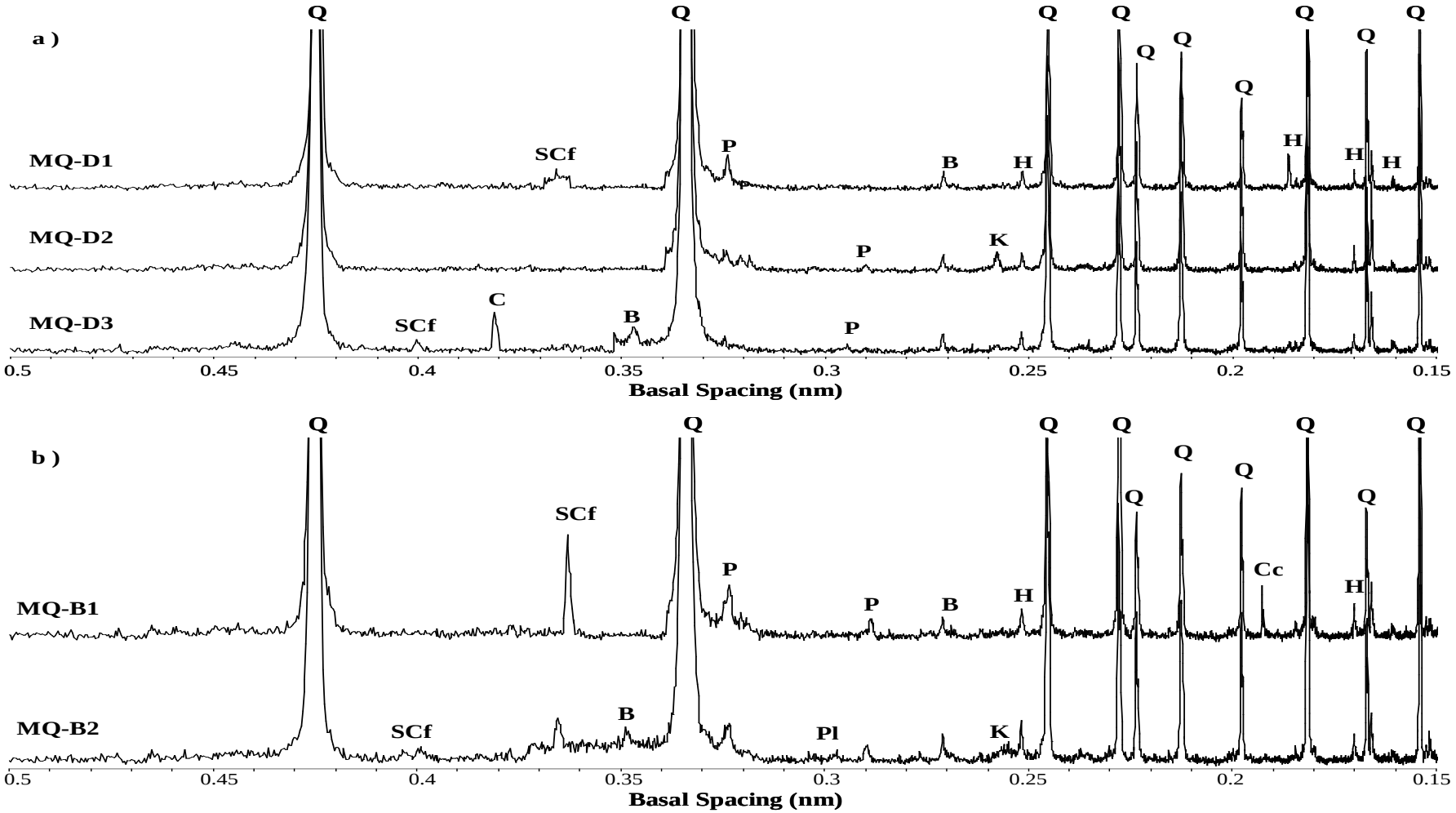

Fig. 12. X-Ray diffractograms of 'dust-sized' fraction from Towac. (a) Towac loessic, (b) Towac basalt. K, Q, B. P, C, Pl, Cc, SCf and H are for kaolin, quartz, brookite, K-feldspar, Ca-feldspar, plagioclase, calcite, Na-Ca-feldspar and hematite respectively)

Appendix 4

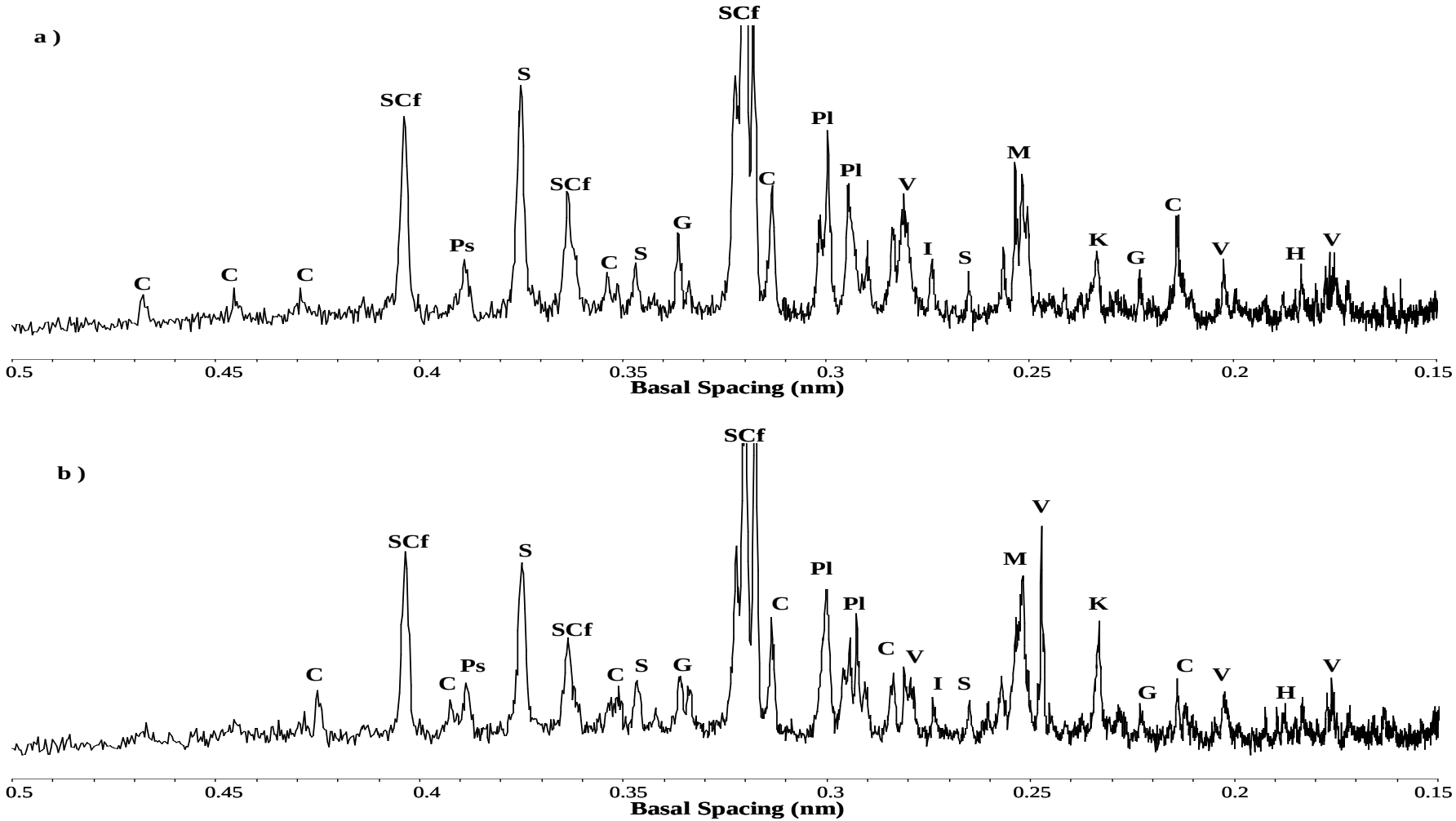

Fig. 13. X-Ray diffractograms of basalt rocks. (a) Huntleys, (b) Cudal. (K, C, Pl, S, SCf, I, Ps, V, G, M and H are for kaolin, Ca-feldspar, plagioclase, Na-feldspar, Na-Ca-feldspar, ilmenite, psilomelane, olivine, goethite, magnetite and hematite respectively.